

Two-pion exchange as a leading-order contribution in chiral effective field theory

Chinmay Mishra,¹ A. Ekström,² G. Hagen,^{3,1} T. Papenbrock,^{1,3} and L. Platter^{1,3,4}

¹*Department of Physics and Astronomy, University of Tennessee, Knoxville, Tennessee 37996, USA*

²*Department of Physics, Chalmers University of Technology, SE-412 96 Göteborg, Sweden*

³*Physics Division, Oak Ridge National Laboratory, Oak Ridge, Tennessee 37831, USA*

⁴*Institut für Kernphysik, Technische Universität Darmstadt, 64289 Darmstadt, Germany*

Pion exchange is the central ingredient to nucleon-nucleon interactions used in nuclear structure calculations, and one pion exchange (OPE) enters at leading order in chiral effective field theory. In the $^{2S+1}L_J = ^1S_0$ partial wave, however, OPE and a contact term needed for proper renormalization fail to produce the qualitative, and quantitative, features of the scattering phase shifts. Cutoff variation also revealed a surprisingly low breakdown momentum $\Lambda_b \approx 330$ MeV in this partial wave. Here we show that potentials consisting of OPE, two pion exchange (TPE), and a single contact address these problems and yield accurate and renormalization group (RG) invariant phase shifts in the 1S_0 partial wave. We demonstrate that a leading-order potential with TPE can be systematically improved by adding a contact quadratic in momenta. For momentum cutoffs $\Lambda \lesssim 500$ MeV, the removal of relevant physics from TPE loops needs to be compensated by additional contacts to keep RG invariance. Inclusion of the Δ isobar degree of freedom in the potential does not change the strong contributions of TPE.

I. INTRODUCTION

Ever since its introduction by Yukawa [1], boson exchange has been central to the theory of nuclear interactions. In quantum chromodynamics, chiral symmetry is spontaneously and explicitly broken, and the pion emerges as the corresponding pseudo Nambu-Goldstone boson. Pion exchange, together with contact interactions that account for unknown short-range physics, thus are the ingredients in a chiral effective field theory (EFT) description of the nucleon-nucleon interaction [2–9].

In chiral EFT, and within the commonly employed Weinberg power counting, the leading-order contributions to the nucleon-nucleon interaction consist of OPE and one contact each in the 1S_0 and 3S_1 partial waves. At next-to-leading order (NLO) in Weinberg counting the leading TPE contributions as well as contacts quadratic in momenta enter.

Statistical analyses of higher-order chiral EFT predictions for nucleon-nucleon scattering data infer a breakdown momentum $\Lambda_b \approx 600 - 700$ MeV, and that higher chiral orders yield systematical improvements in powers of $Q/\min(\Lambda, \Lambda_b)$ beyond the leading-order results [10, 11]. Here Q is the low-momentum scale of interest, e.g., the external momentum in nucleon-nucleon scattering, and Λ is the cutoff employed in the regularization of the theory. While this looks encouraging, there are well-known challenges [12], and we mention two of them.

First, recent results [13–15] show that leading-order chiral EFT potentials predict light-mass nuclei that are unstable with respect to breakup into α particles and lighter-mass clusters, raising questions about what should be expected from a nuclear EFT at leading order. Of course, the lack of any spin-orbit contributions at leading order in the Weinberg power counting would also presumably make well-known nuclear shell-structure a subleading effect.

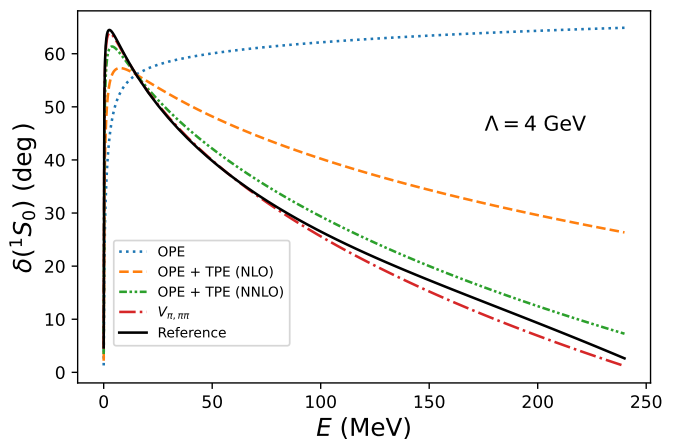


FIG. 1. (Color online) Nucleon-nucleon phase shifts in the 1S_0 partial wave versus the laboratory scattering energy E for various chiral interactions. The momentum cutoff is set to 4 GeV and in all cases a single contact $V_{\text{ct}}^{(0)}$ is adjusted to match the phase shift to that of the reference potential (high-precision Idaho-N3LO) by Entem and Machleidt [16] (solid black line) at $E_0 = 15$ MeV. The dotted blue line shows phase shift obtained for OPE, the dashed orange line for OPE plus the leading TPE, the dash-dot-dotted green line for OPE plus subleading TPE, and the dash-dotted red line for the interaction $V_{\pi,\pi\pi}$ consisting of OPE and leading plus subleading TPE (see text for details).

Second, the leading-order description of nucleon-nucleon phase shifts in the 1S_0 partial wave are problematic in the Weinberg power counting [14, 17–31], see Ref. [32] for a recent review. The combination of OPE and a single contact fails qualitatively to capture the pronounced peak at 60–70 degrees in the phase shift at about 8 MeV of laboratory scattering energy, see blue dotted line in Fig. 1. For all results in this figure, the 1S_0 contact is adjusted to the reference phase shifts of the po-

tential [16] (shown as a solid black line) at a laboratory scattering energy $E = 15$ MeV. This energy matches the relevant scale of pion physics as $m_\pi^2/m_N \approx 20$ MeV using the pion and nucleon mass m_π and m_N , respectively. The OPE phase shifts are much too attractive beyond the matching point and clearly fail to capture the characteristics of the reference phase shifts. Also, the slope of the OPE phase shift has the wrong sign.

Another problem concerns the breakdown momentum Λ_b . The analysis of the 1S_0 phase shifts by Lepage [33] showed that a potential consisting of OPE plus leading and subleading contacts leads to $\Lambda_b \approx 330$ MeV in the 1S_0 partial wave. Later analyses exploring perturbative inclusion of subleading TPE contributions [22, 34] confirmed this finding and estimated the breakdown momentum to be even lower, i.e., $\Lambda_b \approx 200$ MeV. This questions whether leading-order chiral EFT based on OPE physics is consistent with the general assumption that the breakdown momentum is somewhere between ~ 500 and ~ 1000 MeV.

Several researchers addressed the shortcoming of too attractive 1S_0 phase shifts by adding effective-range corrections [14, 35], energy-dependent potentials generated by di-baryon fields [29], or separable potentials [31] to the OPE as leading-order contributions. These approaches improve the phase shifts at a cost of introducing additional parameters. The promotion of TPE to leading order in chiral EFT was proposed already a decade ago by Birse [25], however, a rigorous analysis has (to the best of our knowledge) never been carried out.

In this paper we show that chiral physics in the form of TPE, presumably a higher-order correction in the Weinberg power counting, remedies the shortcomings of highly attractive 1S_0 phase shifts and without increasing the number of parameters. As Fig. 1 shows, the inclusion of TPE at leading order significantly improves the accuracy of the 1S_0 phase shifts. We will also show that the estimated breakdown momentum in this approach is consistent with expectations from chiral EFT.

Phenomenology connects TPE with the strong mid-range attraction of the nucleon-nucleon force [36, 37] which is also attributed to the $f_0(500)$ resonance [38] or the sigma meson whose width and mass was determined model-independently in Ref. [39]. The latter is a central ingredient of relativistic mean-field theories [40–44] and of alternative proposals to chiral EFT which include the effects of the $f_0(500)$ resonance at leading order via the sigma meson [45] or the dilaton [46, 47], i.e. the Nambu-Goldstone boson of a broken and hidden scale symmetry.

In the Weinberg power counting TPE enters at NLO, but its strongest contributions involving the pion-nucleon coupling constants c_i , with $i = 1, 3, 4$, enter at next-to-next-to-leading order (NNLO). It is known that these subleading TPE contributions are crucial for quantitatively reproducing the 1S_0 phase shifts, see, e.g., Refs. [21, 48]. We note, however, that the role of TPE is somewhat obscured in chiral potentials. First, an additional contact potential quadratic in momentum also

enters in the 1S_0 partial wave at NLO in the Weinberg power counting. Second, several popular potentials [16, 49–52] employ relatively low momentum cutoffs and thereby truncate some parts of the TPE strength.

This manuscript is ordered as follows: In Sec. II we give the explicit form of the OPE and TPE potentials, discuss their relative strengths, and show results for phase shifts in the 1S_0 partial wave obtained using the proposed leading-order potential where we have promoted TPE. In Sec. III we show that a subleading contact that is quadratic in momenta systematically improves upon these results. In Sec. IV we show that the inclusion of Δ isobar degrees of freedom does not alter our conclusions about promoting TPE to leading order. We end with a summary in Sec. V.

II. CHIRAL OPE AND TPE POTENTIALS

Canonical chiral EFT descriptions of the nuclear interaction employ a power counting for the pion-nucleon potential as done in chiral perturbation theory. The OPE enters at leading order, and subleading contributions are presumably suppressed by powers of $g_A m_\pi / (4\pi f_\pi) \ll 1$, where $g_A \approx 1.28$ is the axial-vector constant, $m_\pi \approx 140$ MeV is the pion mass, and $f_\pi \approx 92$ MeV is the pion-decay constant. The OPE potential is given by

$$V_{\text{OPE}}(\mathbf{q}) = -\frac{g_A^2}{4f_\pi^2} \boldsymbol{\tau}_1 \cdot \boldsymbol{\tau}_2 \frac{(\boldsymbol{\sigma}_1 \cdot \mathbf{q})(\boldsymbol{\sigma}_2 \cdot \mathbf{q})}{m_\pi^2 + q^2}. \quad (1)$$

Here, $\mathbf{q} = \mathbf{p}' - \mathbf{p}$ is the momentum transfer. The Pauli matrices of nucleon j in spin and isospin space are denoted as σ_j and τ_j , respectively. The TPE potentials considered in this work can be written as

$$\begin{aligned} V_{\text{TPE}}(\mathbf{q}) = & V_C(q) + \boldsymbol{\tau}_1 \cdot \boldsymbol{\tau}_2 W_C(q) \\ & + [V_T(q) + \boldsymbol{\tau}_1 \cdot \boldsymbol{\tau}_2 W_T(q)] (\boldsymbol{\sigma}_1 \cdot \mathbf{q})(\boldsymbol{\sigma}_2 \cdot \mathbf{q}) \\ & + [V_S(q) + \boldsymbol{\tau}_1 \cdot \boldsymbol{\tau}_2 W_S(q)] \boldsymbol{\sigma}_1 \cdot \boldsymbol{\sigma}_2. \end{aligned} \quad (2)$$

The leading TPE potential, i.e., the contributions that enter at NLO in the Weinberg power counting is given by [6, 7, 48]

$$\begin{aligned} W_C = & -\frac{L(q)}{384\pi^2 f_\pi^4} \left[4m_\pi^2 (5g_A^4 - 4g_A^2 - 1) \right. \\ & \left. + q^2 (23g_A^4 - 10g_A^2 - 1) + \frac{48g_A^4 m_\pi^4}{w^2} \right], \quad (3) \\ V_T = & -\frac{V_S}{q^2} = -\frac{3g_A^4 L(q)}{64\pi^2 f_\pi^4}, \end{aligned}$$

while the subleading contributions that enter at NNLO are [6, 7, 48]

$$\begin{aligned} V_C = & -\frac{3g_A^2}{16\pi f_\pi^4} [2m_\pi^2 (2c_1 - c_3) - c_3 q^2] \tilde{w}^2 A(q), \\ W_T = & -\frac{W_S}{q^2} = -\frac{g_A^2}{32\pi f_\pi^4} c_4 w^2 A(q). \end{aligned} \quad (4)$$

Here, we used the short-hands

$$w \equiv \sqrt{4m_\pi^2 + q^2}, \quad (5)$$

$$L(q) \equiv \frac{w}{q} \log \frac{w+q}{2m_\pi}, \quad (6)$$

$$\tilde{w} \equiv \sqrt{2m_\pi^2 + q^2}, \quad (7)$$

$$A(q) \equiv \frac{1}{2q} \arctan \frac{q}{2m_\pi}, \quad (8)$$

with $q \equiv |\mathbf{q}|$, and the pion-nucleon constants c_i are of the order of m_N^{-1} with m_N denoting the nucleon mass m_N . In what follows we use $c_1 = -0.74 \text{ GeV}^{-1}$, $c_3 = -3.61 \text{ GeV}^{-1}$, and $c_4 = 2.44 \text{ GeV}^{-1}$ from Ref. [10], obtained from Roy-Steiner relations [53, 54]. We note here that we have neglected any relativistic corrections (proportional to m_N^{-1}) to the TPE at NNLO, and we have omitted any polynomial contributions.

We evaluated the potentials in the spin-singlet / isospin-triplet partial wave and show their magnitudes in Fig. 2 comparing the OPE, leading TPE, and sub-leading TPE contributions. As expected, OPE is a dominant contribution, while the subleading TPE potential of Eq. (4) cannot be neglected around momentum transfers of about 1 fm^{-1} . Clearly, at momentum transfers of the order of the pion mass ($m_\pi \approx 0.7 \text{ fm}^{-1}$) or the Fermi momentum in nuclear matter at saturation ($k_F \approx 1.35 \text{ fm}^{-1}$), the placement of this TPE potential at NNLO does not reflect its actual strength.

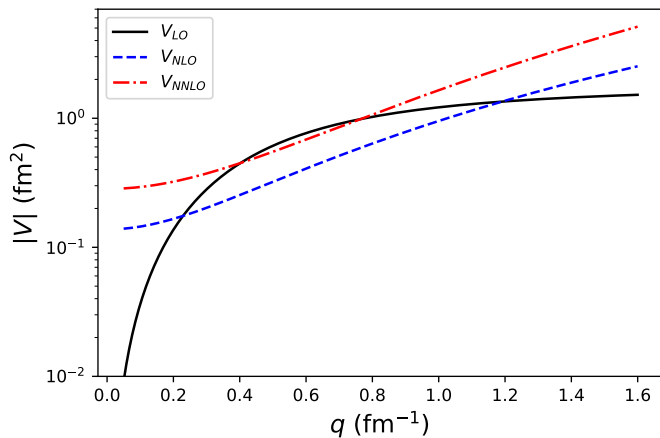


FIG. 2. (Color online) Pion-exchange contributions to the nucleon-nucleon potentials in the spin-singlet / isospin-triplet partial wave at various orders in Weinberg power counting as a function of momentum transfer. The OPE potential (black solid line) is leading order in the Weinberg power counting, the leading TPE (dashed blue line) is NLO, and the sub-leading TPE (dash-dotted red line) enters at NNLO.

Let us study the impact of TPE added to OPE in the 1S_0 phase shifts. We define a nucleon-nucleon potential in this partial wave that is of the form

$$V(\mathbf{p}', \mathbf{p}) \equiv V_{\pi,\pi\pi} + V_{\text{ct}}. \quad (9)$$

Here, $V_{\pi,\pi\pi}$ consists of OPE and the leading and sub-leading TPE, while V_{ct} denotes the contact potential to be specified. At leading order and NLO, the contact potentials are given by

$$V_{\text{ct}}^{(0)}(\mathbf{p}', \mathbf{p}) = \tilde{C}, \quad (10)$$

and

$$V_{\text{ct}}^{(2)}(\mathbf{p}', \mathbf{p}) = C(p'^2 + p^2), \quad (11)$$

respectively. The potentials are regularized via

$$V \rightarrow f(p'^2/\Lambda^2)Vf(p^2/\Lambda^2) \quad (12)$$

using $p \equiv |\mathbf{p}|$, $p' \equiv |\mathbf{p}'|$,

$$f(x) = e^{-x^n}, \quad (13)$$

and $n = 3$. For TPE loop diagrams we use a spectral function regulator with a cutoff of 700 MeV as introduced in [55, 56].

At leading order we adjust the low-energy constant (LEC) \tilde{C} such that the phase shift at the laboratory energy $E_0 = 15 \text{ MeV}$ reproduces the value from the high-precision Idaho-N3LO potential [16], which we take as a reference throughout this work. The precision of this reference is sufficient for our purposes, as the phase shifts of this potential are virtually indistinguishable from a recent partial-wave analysis of nucleon-nucleon scattering data [57].

The 1S_0 phase shifts for our leading-order potential are shown as the red dash-dotted line in Fig. 1. For comparison, we also show the results from potentials with other combinations of pion exchanges; such as the sum of OPE and leading TPE (orange dashed line) and OPE plus subleading TPE (green dash-dot-dotted line). The chiral potential $V_{\pi,\pi\pi}$ stands out through its accuracy for scattering energies below and above the energy E_0 used for renormalizing the contact LEC. This suggests that the combination $V_{\pi,\pi\pi}$ of OPE and TPE should be taken as the leading-order contribution from chiral physics in the 1S_0 partial wave. This is the main result of this paper. It is consistent with the anticipation obtained from Fig. 2. Although the combination of OPE and leading TPE (shown as the orange dashed line) brings the phase shift closer to reference it fails to reproduce the characteristic decrease of the phase shifts with increasing energy, i.e., a lack of increasing repulsion with E , and the amplitude zero is nowhere near $E \approx 250 \text{ MeV}$. In contrast, using $V_{\pi,\pi\pi}$ leads to a leading-order nucleon-nucleon potential that captures the main qualitative and quantitative features of the 1S_0 phase shifts.

We note that the phase shifts presented in Fig. 1 include chiral physics plus a single LEC that accounts for unknown short-range physics. Figure 3 demonstrates that the potential $V_{\pi,\pi\pi} + V_{\text{ct}}^{(0)}$ yields RG invariant 1S_0 phase shifts as the cutoff Λ is increased. For a comparison, the reference phase shifts are shown as black stars.

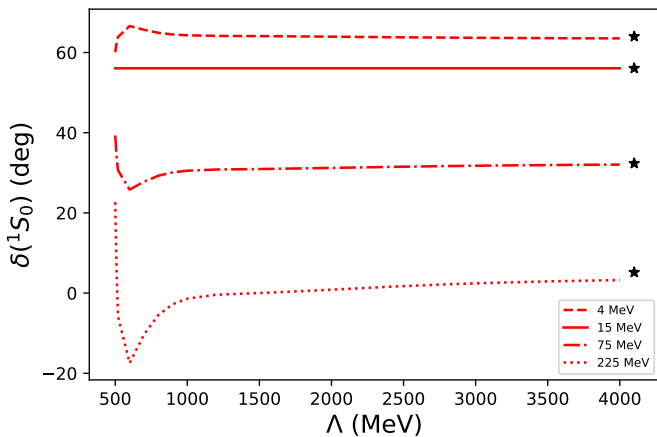


FIG. 3. (Color online) 1S_0 phase shifts as a function of the momentum regulator cutoff Λ at laboratory energies of $E = 4$ (dashed), 15 (solid), 75 (dash-dotted), and 225 MeV (dotted) for the potential $V_{\pi,\pi\pi} + V_{\text{ct}}^{(0)}$. The black stars show the reference phase shifts at these energies.

Figure 3 also shows that the phase shifts are strongly cutoff dependent for $\Lambda \lesssim 750$ MeV. This can be understood as follows: In coordinate space, the OPE potential exhibits a $1/r^3$ behavior at short distances, where r denotes the two-nucleon relative distance. The TPE potential exhibits a significantly more singular $1/r^6$ short-distance behavior with a typical momentum scale $k_{\pi\pi} \sim 115$ MeV set by the chiral couplings employed in the TPE potential [34]. The cutoff needs therefore to be significantly larger than $k_{\pi\pi}$ to reach convergence. Alternatively, the relevant scale of the TPE interaction can also naively be estimated by

$$\Lambda_{\text{TPE}} \equiv \sqrt{2m_{\pi}m_N} \approx 510 \text{ MeV}. \quad (14)$$

Cutoffs lower than Λ_{TPE} therefore remove physics from the TPE. This effect is highlighted in Fig. 4. As before, we adjusted the leading-order contact $V_{\text{ct}}^{(0)}$ to reproduce the reference phase shift at $E_0 = 15$ MeV. We clearly see the effects of removing TPE physics for cutoffs $\Lambda \lesssim 500$ MeV. Indeed, comparison with Fig. 1 shows that the phase shifts at a cutoff of $\Lambda = 475$ MeV are close to those of OPE plus a contact. As we will see below, adding the subleading contact $V_{\text{ct}}^{(2)}$ will restore RG invariance in this case.

Figure 4 also allows us to estimate the breakdown momentum in this partial wave as the momentum regulator cutoff value for which the phase shift predictions are closest to the reference [33]. Following this strategy we infer $\Lambda_b \approx 500 - 520$ MeV. This is significantly larger than what was found when only OPE physics is included at leading order [22, 33, 34]. It is also in line with expectations from neglecting the physics of more massive exchange mesons.

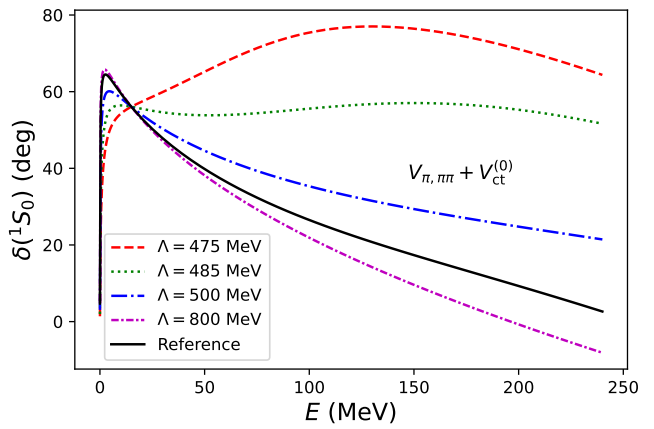


FIG. 4. (Color online) Phase shifts as a function of laboratory energy of the interaction $V_{\pi,\pi\pi} + V_{\text{ct}}^{(0)}$ at low momentum cutoffs as indicated and compared to the reference (solid black line). The phase shifts become increasingly repulsive as the cutoff is increased. For $E > 15$ MeV they cross over and become more repulsive than the reference for cutoffs in the range $500 \lesssim \Lambda \lesssim 520$ MeV.

III. SYSTEMATIC IMPROVEMENTS

We propose to employ higher-order contacts to systematically improve upon the results of our leading-order potential $V_{\pi,\pi\pi} + V_{\text{ct}}^{(0)}$. Thus, the contact (11) enters as the subleading correction [33]. This introduces a new LEC, C , and we adjust \tilde{C} and C such that the reference phase shift and its slope is reproduced at the laboratory energy $E_0 = 15$ MeV. In our numerical work, we used the secant slope between E_0 and a second point just below this energy rather than the exact tangent slope. We work at a cutoff of $\Lambda = 800$ MeV.

The question then arises whether one should treat the subleading correction perturbatively, or not. In the non-perturbative approach, the full potential is iterated to solve the Lippmann Schwinger equation, while the perturbative approach is linear in the subleading correction. We followed both approaches and found similar results for the phase shifts.

Let us discuss the non-perturbative approach. A simultaneous fit of the two LECs (\tilde{C}, C) to the phase shift and its slope at E_0 is somewhat challenging. Instead, we first calibrated \tilde{C} and subsequently determined C such that the reference phase shift is reproduced at E_0 . Repeating this procedure for various values of \tilde{C} yields a one-parameter curve $C(\tilde{C})$. Interestingly, we found that this is a quadratic function to very high accuracy. We then moved along this parabola and determined the point where the slope of the phase shift agrees with the reference as well. The resulting phase shifts are shown as a dashed blue line in Fig. 5 and compared to our leading-order results (red dash-dotted line). The improvement is clearly visible. Figure 6 shows the absolute differences between our phase shifts and the reference on

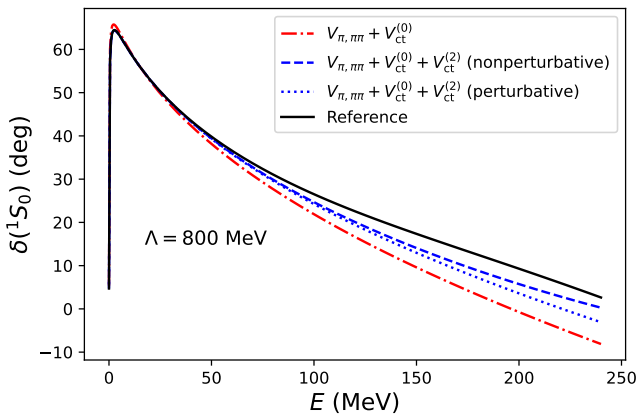


FIG. 5. (Color online) Systematic improvements of the 1S_0 phase shifts by adding the subleading contact $V_{ct}^{(2)}$ to the potential $V_{\pi, \pi\pi} + V_{ct}^{(0)}$. The cutoff is 800 MeV. Results for the potentials $V_{\pi, \pi\pi} + V_{ct}^{(0)}$ and $V_{\pi, \pi\pi} + V_{ct}^{(0)} + V_{ct}^{(2)}$ are shown as a dash-dotted red line and as blue lines, respectively. The dashed and the dotted blue line correspond to the non-perturbative and the perturbative inclusion of the subleading contact $V_{ct}^{(2)}$, respectively, and the solid black line shows the reference.

a log-log plot. The systematic power-law improvement from the quadratic contact is evident. We also note that $C\Lambda_b^2/\tilde{C} \approx -4$, and this is consistent with expectations from naive dimensional analysis where this dimensionless number should be $\mathcal{O}(1)$ in size.

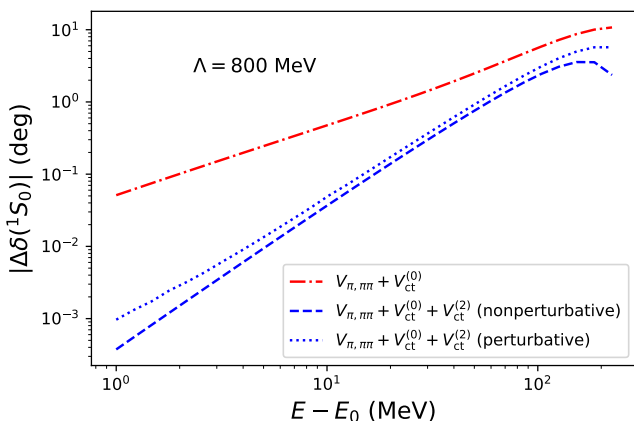


FIG. 6. (Color online) Log-log plot of absolute differences to the reference phase shifts versus the energy difference to the matching point. The cutoff is 800 MeV. Results for the potentials $V_{\pi, \pi\pi} + V_{ct}^{(0)}$ and $V_{\pi, \pi\pi} + V_{ct}^{(0)} + V_{ct}^{(2)}$ are shown as dash-dotted red and as blue lines, respectively. The dashed and the dotted blue line correspond to the non-perturbative and the perturbative inclusion of the subleading contact $V_{ct}^{(2)}$, respectively.

In a second approach, we treated the contact (11) in perturbation theory. Our leading-order theory is adjusted to the reference phase shift at E_0 and the cor-

responding LECs are $(\tilde{C}, C) = (\tilde{C}_0, 0)$. In a perturbative approach the LECs become $(\tilde{C}_0 + \delta\tilde{C}, \delta C)$ in presence of the potential $V_{ct}^{(2)}$. We expand the phase shift as

$$\delta(E) \approx \delta(E)|_0 + \left. \frac{\partial\delta(E)}{\partial\tilde{C}} \right|_0 \delta\tilde{C} + \left. \frac{\partial\delta(E)}{\partial C} \right|_0 \delta C \quad (15)$$

Here, the subscript 0 implies that all functions are evaluated at $(\tilde{C}_0, 0)$. We determine the derivatives numerically. Keeping the phase shift at E_0 unchanged implies

$$\left. \frac{\partial\delta(E_0)}{\partial\tilde{C}} \right|_0 \delta\tilde{C} + \left. \frac{\partial\delta(E_0)}{\partial C} \right|_0 \delta C = 0, \quad (16)$$

and, thus, a linear relation between $\delta\tilde{C}$ and δC . A one-parameter search along this line yields the optimal point that also reproduces the slope of the reference phase shifts at E_0 . We then compute the resulting phase shifts using Eq. (15). The corresponding results are shown as blue dotted lines in Figs. 5 and 6. We see that the perturbative and non-perturbative solutions phase shifts are close to each other, and that both yield a power-law improvement of our leading-order results. We also note that $\Lambda_b^2\delta C/(\tilde{C}_0 + \delta C) \approx -0.03$, and this is smaller in magnitude than expected from naive dimensional analysis.

We also revisited the low cutoffs at and below the scale Λ_{TPE} in Eq. (14) and employed the subleading contact $V_{ct}^{(2)}$ in Eq. (11) non-perturbatively by matching the phase shift and its slope to the reference at a laboratory energy of 15 MeV. The results are shown in Fig. 7 and comparison with Fig. 4 shows that RG invariance is restored also at low momentum cutoffs.

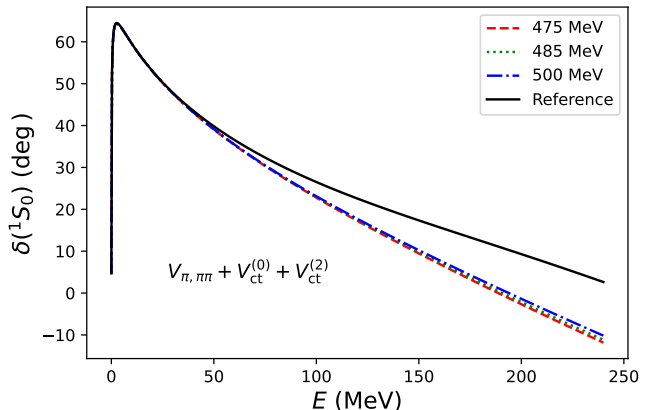


FIG. 7. (Color online) The 1S_0 phase shifts as a function of the laboratory energy E with the interaction $V_{\pi, \pi\pi} + V_{ct}^{(0)} + V_{ct}^{(2)}$ at low cutoffs as indicated and compared to the reference (solid black line). The additional contact $V_{ct}^{(2)}$ restores the RG invariance that was lacking in Fig. 4.

IV. THE ROLE OF Δ ISOBAR DEGREES OF FREEDOM

The strong contributions of the subleading TPE in chiral EFT, i.e., the relatively large values of the pion-nucleon LECs c_i , are usually attributed to “resonance saturation.” Consequently, these couplings become more natural in size when the Δ isobar degrees of freedom are included. Notably, such chiral EFTs have TPE terms that involve a Δ excitation already at NLO in the Weinberg power counting. The corresponding expressions for the potentials (2) were derived by Kaiser *et al.* [58] and we use those published by Krebs *et al.* [59] in their Eqs. (2.5) to (2.8). The chiral potential we employ thus consists of the OPE [given in Eq. (1)], leading TPE [given in Eq. (3)], the contact (10), and the leading Δ contributions to TPE. In our numerical implementation this potential is regularized with $n = 4$ in the regulator (13) and spectral-function regularization was used with a cutoff of $\Lambda = 700$ MeV.

We repeated the calculations presented above and found very similar results regarding the quality of the phase shifts in the 1S_0 partial wave, a breakdown momentum $\Lambda_b \approx 500$ MeV, and a systematic power-law improvement when the contact (11) quadratic in momenta is included. An example is shown in Fig. 8, to be compared with Fig. 5.

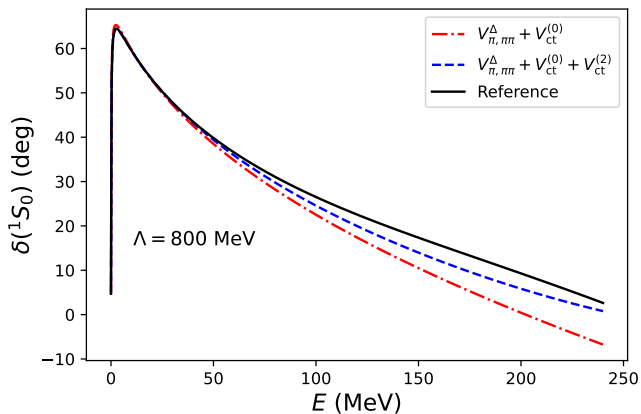


FIG. 8. (Color online) The 1S_0 phase shifts as a function of the laboratory energy E for the $V_{\pi, \pi\pi}^\Delta$ interaction, i.e., our leading-order potential with Δ isobars included in the leading TPE potential. The dash-dotted red line uses a single contact $V_{ct}^{(0)}$ to reproduce the value of the reference phase shift at $E_0 = 15$ MeV. The dashed blue line shows the phase shift when leading and subleading contacts $V_{ct}^{(0)} + V_{ct}^{(2)}$ are fit to reproduce the value and the slope of the reference phase shift at E_0 . The cutoff is 800 MeV, and the reference phase shifts are shown as a solid black line. The results are close to those shown in Fig. 5.

V. SUMMARY AND DISCUSSION

We analyzed chiral EFT in the 1S_0 partial wave and propose to promote leading and subleading TPE to accompany OPE along with a single contact $V_{ct}^{(0)}$ at leading order. Naturally, power counting in EFT applies to observables or amplitudes. Nevertheless, the promotion of TPE to leading order is inspired by the unexpectedly large matrix elements of the TPE potential that formally enter at NNLO in the Weinberg power counting. We find that our leading-order interaction cures two problems with the standard approach. First, the phase shifts in the 1S_0 partial wave are accurately reproduced and RG invariant for scattering energies of the order m_π^2/m_N and for large cutoffs. Second, the estimated breakdown momentum $\Lambda_b \approx 500$ MeV in 1S_0 is consistent with assumptions from chiral EFT. We also showed that adding a contact quadratic in momenta as a subleading correction leads to a systematic power-law improvement of the phase shifts. We find that including the leading Δ contributions to TPE as a new leading-order contribution achieves the same. We expect that additional and smaller pion contributions and higher-order contacts to yield additional and systematic power-law improvements. We also pointed out that chiral EFTs with cutoffs below about 500 MeV are really “two-pion-less” EFTs as they cut off parts of the TPE; in such cases higher-order contacts are needed for maintaining proper RG invariance.

ACKNOWLEDGMENTS

We thank Daniel Phillips for insightful and useful discussions. We also thank the participants of the INT program “Nuclear Forces for Precision Nuclear Physics (21-1b)” for many useful exchanges and discussions. This material is based upon work supported by the U.S. Department of Energy, Office of Science, Office of Nuclear Physics under award numbers DE-FG02-96ER40963 and DE-SC0018223 (NUCLEI SciDAC-4 collaboration), and contract No. DE-AC05-00OR22725 with UT-Battelle, LLC (Oak Ridge National Laboratory), the Swedish Research Council grant number 2020-005127, the European Research Council (ERC) under the European Union’s Horizon 2020 research and innovation programme (grant agreement number 758027), by the Deutsche Forschungsgemeinschaft (DFG, German Research Foundation) – Projektnummer 279384907 – CRC 1245. and by the National Science Foundation under Grant Nos. PHY-1555030 and PHY-2111426.

[1] H. Yukawa, On the interaction of elementary particles. i, Proceedings of the Physico-Mathematical Society of

Japan. 3rd Series **17**, 48 (1935).

- [2] S. Weinberg, Nuclear forces from chiral lagrangians, *Phys. Lett. B* **251**, 288 (1990).
- [3] S. Weinberg, Effective chiral lagrangians for nucleon-pion interactions and nuclear forces, *Nuclear Physics B* **363**, 3 (1991).
- [4] C. Ordóñez and U. van Kolck, Chiral lagrangians and nuclear forces, *Phys. Lett. B* **291**, 459 (1992).
- [5] U. van Kolck, Few-nucleon forces from chiral Lagrangians, *Phys. Rev. C* **49**, 2932 (1994).
- [6] N. Kaiser, R. Brockmann, and W. Weise, Peripheral nucleon-nucleon phase shifts and chiral symmetry, *Nucl. Phys. A* **625**, 758 (1997).
- [7] E. Epelbaum, W. Glöckle, and U.-G. Meißner, Nuclear forces from chiral lagrangians using the method of unitary transformation ii: The two-nucleon system, *Nucl. Phys. A* **671**, 295 (2000).
- [8] E. Epelbaum, H.-W. Hammer, and U.-G. Meißner, Modern theory of nuclear forces, *Rev. Mod. Phys.* **81**, 1773 (2009).
- [9] H. W. Hammer, S. König, and U. van Kolck, Nuclear effective field theory: status and perspectives, *Rev. Mod. Phys.* **92**, 025004 (2020), arXiv:1906.12122 [nucl-th].
- [10] P. Reinert, H. Krebs, and E. Epelbaum, Semilocal momentum-space regularized chiral two-nucleon potentials up to fifth order, *The European Physical Journal A* **54**, 86 (2018).
- [11] S. Wesolowski, R. J. Furnstahl, J. A. Melendez, and D. R. Phillips, Exploring bayesian parameter estimation for chiral effective field theory using nucleon–nucleon phase shifts, *Journal of Physics G: Nuclear and Particle Physics* **46**, 045102 (2019).
- [12] R. J. Furnstahl, H. W. Hammer, and A. Schwenk, Nuclear Structure at the Crossroads, *Few-Body Systems* **62**, 72 (2021).
- [13] B. D. Carlsson, A. Ekström, C. Forssén, D. F. Strömberg, G. R. Jansen, O. Lilja, M. Lindby, B. A. Mattsson, and K. A. Wendt, Uncertainty analysis and order-by-order optimization of chiral nuclear interactions, *Phys. Rev. X* **6**, 011019 (2016).
- [14] C.-J. Yang, A. Ekström, C. Forssén, and G. Hagen, Power counting in chiral effective field theory and nuclear binding, *Phys. Rev. C* **103**, 054304 (2021).
- [15] P. Maris, E. Epelbaum, R. J. Furnstahl, J. Golak, K. Hebeler, T. Hüther, H. Kamada, H. Krebs, U.-G. Meißner, J. A. Melendez, A. Nogga, P. Reinert, R. Roth, R. Skibiński, V. Soloviov, K. Topolnicki, J. P. Vary, Y. Volkotrub, H. Witała, and T. Wolfgruber (LENPIC Collaboration), Light nuclei with semilocal momentum-space regularized chiral interactions up to third order, *Phys. Rev. C* **103**, 054001 (2021).
- [16] D. R. Entem and R. Machleidt, Accurate charge-dependent nucleon-nucleon potential at fourth order of chiral perturbation theory, *Phys. Rev. C* **68**, 041001 (2003).
- [17] D. B. Kaplan, M. J. Savage, and M. B. Wise, A new expansion for nucleon-nucleon interactions, *Physics Letters B* **424**, 390 (1998).
- [18] T. Frederico, V. S. Timoteo, and L. Tomio, Renormalization of the one pion exchange interaction, *Nucl. Phys. A* **653**, 209 (1999), arXiv:nucl-th/9902052.
- [19] A. Nogga, R. G. E. Timmermans, and U. v. Kolck, Renormalization of one-pion exchange and power counting, *Phys. Rev. C* **72**, 054006 (2005).
- [20] M. P. Valderrama and E. R. Arriola, Renormalization of the deuteron with one pion exchange, *Phys. Rev. C* **72**, 054002 (2005).
- [21] M. Pavón Valderrama and E. R. Arriola, Renormalization of the NN interaction with a chiral two-pion-exchange potential: Central phases and the deuteron, *Phys. Rev. C* **74**, 054001 (2006).
- [22] M. C. Birse, Power counting with one-pion exchange, *Phys. Rev. C* **74**, 014003 (2006).
- [23] D. Shukla, D. R. Phillips, and E. Mortenson, Chiral potentials, perturbation theory and the 1s_0 channel of NN scattering, *Journal of Physics G: Nuclear and Particle Physics* **35**, 115009 (2008).
- [24] C.-J. Yang, C. Elster, and D. R. Phillips, Subtractive renormalization of the NN scattering amplitude at leading order in chiral effective theory, *Phys. Rev. C* **77**, 014002 (2008).
- [25] M. C. Birse, Deconstructing 1S_0 nucleon-nucleon scattering, *European Physical Journal A* **46**, 231 (2010).
- [26] B. Long and C.-J. Yang, Short-range nuclear forces in singlet channels, *Phys. Rev. C* **86**, 024001 (2012).
- [27] B. Long and C.-J. Yang, Renormalizing chiral nuclear forces: Triplet channels, *Phys. Rev. C* **85**, 034002 (2012).
- [28] M. P. Valderrama and D. R. Phillips, Power counting of contact-range currents in effective field theory, *Phys. Rev. Lett.* **114**, 082502 (2015).
- [29] M. Sánchez Sánchez, C.-J. Yang, B. Long, and U. van Kolck, Two-nucleon 1s_0 amplitude zero in chiral effective field theory, *Phys. Rev. C* **97**, 024001 (2018).
- [30] D. Odell, A. Deltuva, J. Bonilla, and L. Platter, Renormalization of a finite-range inverse-cube potential, *Phys. Rev. C* **100**, 054001 (2019).
- [31] M. Sánchez Sánchez, N. A. Smirnova, A. M. Shirokov, P. Maris, and J. P. Vary, Improved description of light nuclei through chiral effective field theory at leading order, *Phys. Rev. C* **102**, 024324 (2020).
- [32] U. van Kolck, The problem of renormalization of chiral nuclear forces, *Frontiers in Physics* **8**, 79 (2020).
- [33] G. P. Lepage, How to renormalize the Schrödinger equation, in *8th Jorge Andre Swieca Summer School on Nuclear Physics* (1997) arXiv:nucl-th/9706029.
- [34] M. Pavón Valderrama, Perturbative renormalizability of chiral two-pion exchange in nucleon-nucleon scattering, *Phys. Rev. C* **83**, 024003 (2011).
- [35] E. Epelbaum, A. M. Gasparyan, J. Gegelia, and H. Krebs, 1S_0 nucleon-nucleon scattering in the modified Weinberg approach, *Eur. Phys. J. A* **51**, 71 (2015).
- [36] R. B. Wiringa, V. G. J. Stoks, and R. Schiavilla, Accurate nucleon-nucleon potential with charge-independence breaking, *Phys. Rev. C* **51**, 38 (1995).
- [37] R. Machleidt, High-precision, charge-dependent Bonn nucleon-nucleon potential, *Phys. Rev. C* **63**, 024001 (2001).
- [38] J. R. Peláez, From controversy to precision on the sigma meson: A review on the status of the non-ordinary $f_0(500)$ resonance, *Physics Reports* **658**, 1 (2016).
- [39] I. Caprini, G. Colangelo, and H. Leutwyler, Mass and width of the lowest resonance in QCD, *Phys. Rev. Lett.* **96**, 132001 (2006), arXiv:hep-ph/0512364.
- [40] J. D. Walecka, The relativistic nuclear many-body problem, in *New Vistas in Nuclear Dynamics*, NATO ASI Series (Series B: Physics), Vol. 139, edited by P. J. Busza and J. H. Koch (Springer, Boston, MA, 1986) pp. 229–271.

- [41] P.-G. Reinhard, The relativistic mean-field description of nuclei and nuclear dynamics, Reports on Progress in Physics **52**, 439 (1989).
- [42] Y. K. Gambhir, P. Ring, and A. Thimet, Relativistic mean field theory for finite nuclei, Annals of Physics **198**, 132 (1990).
- [43] B. D. Serot and J. D. Walecka, Relativistic nuclear many-body theory, in *Recent Progress in Many-Body Theories*, edited by T. L. Ainsworth, C. E. Campbell, B. E. Clements, and E. Krotscheck (Springer, Boston, MA, 1992) pp. 49–92.
- [44] Y. Sugahara and H. Toki, Relativistic mean-field theory for unstable nuclei with non-linear σ and ω terms, Nuclear Physics A **579**, 557 (1994).
- [45] J. F. Donoghue, Sigma exchange in the nuclear force and effective field theory, Physics Letters B **643**, 165 (2006).
- [46] R. J. Crewther and L. C. Tunstall, $\Delta I = 1/2$ rule for kaon decays derived from QCD infrared fixed point, Phys. Rev. D **91**, 034016 (2015).
- [47] Y.-L. Ma and M. Rho, Towards the hadron–quark continuity via a topology change in compact stars, Progress in Particle and Nuclear Physics **113**, 103791 (2020).
- [48] R. Machleidt and D. Entem, Chiral effective field theory and nuclear forces, Physics Reports **503**, 1 (2011).
- [49] A. Ekström, G. Baardsen, C. Forssén, G. Hagen, M. Hjorth-Jensen, G. R. Jansen, R. Machleidt, W. Nazarewicz, T. Papenbrock, J. Sarich, and S. M. Wild, Optimized chiral nucleon-nucleon interaction at next-to-next-to-leading order, Phys. Rev. Lett. **110**, 192502 (2013).
- [50] A. Ekström, G. R. Jansen, K. A. Wendt, G. Hagen, T. Papenbrock, B. D. Carlsson, C. Forssén, M. Hjorth-Jensen, P. Navrátil, and W. Nazarewicz, Accurate nuclear radii and binding energies from a chiral interaction, Phys. Rev. C **91**, 051301 (2015).
- [51] D. R. Entem, N. Kaiser, R. Machleidt, and Y. Nosyk, Peripheral nucleon-nucleon scattering at fifth order of chiral perturbation theory, Phys. Rev. C **91**, 014002 (2015).
- [52] W. G. Jiang, A. Ekström, C. Forssén, G. Hagen, G. R. Jansen, and T. Papenbrock, Accurate bulk properties of nuclei from $a = 2$ to ∞ from potentials with Δ isobars, Phys. Rev. C **102**, 054301 (2020).
- [53] M. Hoferichter, J. Ruiz de Elvira, B. Kubis, and U.-G. Meißner, Matching pion-nucleon Roy-Steiner equations to chiral perturbation theory, Phys. Rev. Lett. **115**, 192301 (2015).
- [54] M. Hoferichter, J. Ruiz de Elvira, B. Kubis, and U.-G. Meißner, Roy-Steiner-equation analysis of pion-nucleon scattering, Phys. Rept. **625**, 1 (2016).
- [55] E. Epelbaum, W. Glöckle, and U.-G. Meißner, Improving the convergence of the chiral expansion for nuclear forces. 1. Peripheral phases, Eur. Phys. J. A **19**, 125 (2004), arXiv:nucl-th/0304037.
- [56] E. Epelbaum, W. Glöckle, and U.-G. Meißner, Improving the convergence of the chiral expansion for nuclear forces - ii: Low phases and the deuteron, Eur. Phys. J. A **19**, 401 (2004).
- [57] R. N. Pérez, J. E. Amaro, and E. R. Arriola, Coarse-grained potential analysis of neutron-proton and proton-proton scattering below the pion production threshold, Phys. Rev. C **88**, 064002 (2013).
- [58] N. Kaiser, S. Gerstendörfer, and W. Weise, Peripheral nn-scattering: role of delta-excitation, correlated two-pion and vector meson exchange, Nucl. Phys. A **637**, 395 (1998).
- [59] H. Krebs, E. Epelbaum, and U. G. Meißner, Nuclear forces with Δ excitations up to next-to-next-to-leading order, part i: Peripheral nucleon-nucleon waves, Eur. Phys. J. A **32**, 127 (2007).